

A peer-reviewed version of this preprint was published in PeerJ on 25 November 2015.

[View the peer-reviewed version](https://peerj.com/articles/cs-36) (peerj.com/articles/cs-36), which is the preferred citable publication unless you specifically need to cite this preprint.

Fachada N, Lopes VV, Martins RC, Rosa AC. (2015) Towards a standard model for research in agent-based modeling and simulation. PeerJ Computer Science 1:e36 <https://doi.org/10.7717/peerj-cs.36>

Towards a standard model for research in agent-based modeling and simulation

Nuno Fachada, Vitor V Lopes, Rui C Martins, Agostinho C Rosa

Agent-based modeling (ABM) is a bottom-up modeling approach, where each entity of the system being modeled is uniquely represented as an independent decision-making agent. ABMs are very sensitive to implementation details. Thus, it is very easy to inadvertently introduce changes which modify model dynamics. Such problems usually arise due to the lack of transparency in model descriptions, which constrains how models are assessed, implemented and replicated. In this paper, we present PPHPC, a model which aims to serve as a standard in agent based modeling research, namely, but not limited to, conceptual model specification, statistical analysis of simulation output, model comparison and parallelization studies. This paper focuses on the first two aspects (conceptual model specification and statistical analysis of simulation output), also providing a canonical implementation of PPHPC. The paper serves as a complete reference to the presented model, and can be used as a tutorial for simulation practitioners who wish to improve the way they communicate their ABMs.

Towards a standard model for research in agent-based modeling and simulation

Nuno Fachada¹, Vitor V. Lopes², Rui C. Martins³, and Agostinho C. Rosa⁴

^{1,4}Institute for Systems and Robotics, LARSyS, Instituto Superior Técnico, Universidade de Lisboa, Lisboa, Portugal

²Universidad de las Fuerzas Armadas-ESPE, Sangolquí, Ecuador

³Life and Health Sciences Research Institute, School of Health Sciences, University of Minho, Braga, Portugal

ABSTRACT

Agent-based modeling (ABM) is a bottom-up modeling approach, where each entity of the system being modeled is uniquely represented as an independent decision-making agent. ABMs are very sensitive to implementation details. Thus, it is very easy to inadvertently introduce changes which modify model dynamics. Such problems usually arise due to the lack of transparency in model descriptions, which constrains how models are assessed, implemented and replicated. In this paper, we present PPHPC, a model which aims to serve as a standard in agent based modeling research, namely, but not limited to, conceptual model specification, statistical analysis of simulation output, model comparison and parallelization studies. This paper focuses on the first two aspects (conceptual model specification and statistical analysis of simulation output), also providing a canonical implementation of PPHPC. The paper serves as a complete reference to the presented model, and can be used as a tutorial for simulation practitioners who wish to improve the way they communicate their ABMs.

Keywords: agent-based modeling, standard model, statistical analysis of simulation output, ODD

INTRODUCTION

Agent-based modeling (ABM) is a bottom-up modeling approach, where each entity of the system being modeled is uniquely represented as an independent decision-making agent. When prompted to act, each agent analyzes its current situation (e.g. what resources are available, what other agents are in the neighborhood), and acts appropriately, based on a set of rules. These rules express knowledge or theories about the respective low-level components. The global behavior of the system is the result from the simple, self-organized local relationships between the agents (Fachada, 2008). As such, ABM is a useful tool in simulating and exploring systems that can be modeled in terms of interactions between individual entities, e.g., biological cell cultures, ants foraging for food or military units in a battlefield (Macal and North, 2008). In practice, ABM can be considered a variation of discrete-event simulation, since state changes occur at specific points in time (Law, 2015).

Spatial agent-based models (SABMs) are a subset of ABMs in which a spatial topology defines how agents interact (Shook et al., 2013). For example, an agent may be limited to interact with agents located within a specific radius, or may only move to a near physical or geographical location (Macal and North, 2010). SABMs have been extensively used to study a range of phenomena in the biological and social sciences (Isaac, 2011; Shook et al., 2013).

ABMs are very sensitive to implementation details: the impact that seemingly unimportant aspects such as data structures, algorithms, discrete time representation, floating point arithmetic or order of events can have on results is tremendous (Wilensky and Rand, 2007; Merlone et al., 2008). As such, it is very easy to inadvertently introduce changes which will alter model dynamics. These type of issues usually derive from a lack of transparency in model descriptions, which constrains how models are assessed and implemented (Müller et al., 2014). Conceptual models should be well specified and adequately described in order to be properly implemented and replicated (Edmonds and Hales, 2003; Wilensky and Rand, 2007).

36 The ODD protocol (Overview, Design concepts, Details) is currently one of the most widely used
37 templates for making model descriptions more understandable and complete, providing a comprehensive
38 checklist that covers virtually all the key features that can define a model (Grimm et al., 2010). It allows
39 modelers to communicate their models using a natural language description within a prescriptive and
40 hierarchical structure, aiding in model design and fostering in-depth model comprehension (Müller et al.,
41 2014). It is the recommended approach for documenting models in the CoMSES Net Computational
42 Model Library (Rollins et al., 2014). However, Müller et al. (2014) argue that no single model description
43 standard can completely and thoroughly characterize a model by itself, suggesting that besides a structured
44 natural language description such as ODD, the availability of a model's source code should be part of a
45 minimum standard for model communication. Furthermore, the ODD protocol does not deal with models
46 from a results or simulation output perspective, which means that an additional section for statistical
47 analysis of results is often required. In practice, however, the situation is very different. While many
48 ABMs have been published and simulation output analysis is a widely discussed subject matter (Sargent,
49 1976; Kelton, 1997; Law, 2007; Nakayama, 2008; Law, 2015), comprehensive inquiries concerning the
50 output of ABM simulations are hard to find in the scientific literature.

51 In this paper, we present PPHPC (Predator-Prey for High-Performance Computing), a conceptual
52 model which captures important characteristics of SABMs, such as agent movement and local agent
53 interactions. It aims to serve as a standard in agent based modeling research, and was designed with
54 several goals in mind:

- 55 1. Provide a basis for a tutorial on complete model specification and thorough simulation output
56 analysis.
- 57 2. Investigate statistical comparison strategies for model replication (Fachada et al., 2015a).
- 58 3. Compare different implementations from a performance point of view, using different frameworks,
59 programming languages, hardware and/or parallelization strategies, while maintaining statistical
60 equivalence among implementations (Fachada et al., 2015b).
- 61 4. Test the influence of different pseudo-random number generators (PRNGs) on the statistical accuracy
62 of simulation output.

63 This paper aims to fulfill the first of these goals, and is organized as follows. First, in 'Background', we
64 review several paradigmatic ABMs, as well as model description and analysis. Next, the 'Methodology'
65 section is divided into five subsections, in which we: a) formalize the conceptual model using the ODD
66 protocol; b) describe the canonical PPHPC realization implemented with the NetLogo ABM toolkit
67 (Wilensky, 1999); c) discuss how to select output focal measures; d) explain how to collect and prepare
68 data for statistical analysis; and, e) propose how to analyze focal measures from a statistical point-of-view.
69 In 'Results', statistical analysis of output of the NetLogo implementation is performed. A discussion on
70 how these results can be utilized in additional investigations is undertaken in 'Discussion'. 'Conclusions'
71 provides a global outline of what was accomplished in this paper.

72 BACKGROUND

73 Several ABMs have been used for the purpose of modeling tutorials and/or model analysis and replication.
74 Probably, the most well known standard ABM is the "StupidModel", which consists of a series of 16
75 pseudo-models of increasing complexity, ranging from simple moving agents to a full predator-prey-like
76 model. It was developed by Railsback et al. (2005) as a teaching tool and template for real applications,
77 as it includes a set of features commonly used in ABMs of real systems. It has been used to address a
78 number of questions, including the comparison of ABM platforms (Railsback et al., 2006; Lytinen and
79 Railsback, 2012), model parallelization (Lysenko and D'Souza, 2008; Tang and Wang, 2009), analysis of
80 toolkit feasibility (Standish, 2008) and/or creating models as compositions of micro-behaviors (Kahn,
81 2007). The "StupidModel" series has been criticized for having some atypical elements and ambiguities
82 (Lytinen and Railsback, 2012), reasons which lead Isaac (2011) to propose a reformulation to address
83 these and other issues. However, its multiple versions and user-interface/visualization goals limit the
84 series appeal as a pure computational model for the goals described in the introduction.

85 Other paradigmatic models which have been recurrently used, studied and replicated include Sug-
86 arcscape (Epstein and Axtell, 1996; Axtell et al., 1996; Bigbee et al., 2007; D'Souza et al., 2007; Lysenko

87 and D'Souza, 2008), Heatbugs (Wilensky, 2004; Sallach and Mellarkod, 2005; Goldsby and Pancerella,
88 2013), Boids (Reynolds, 1987, 2006; Goldsby and Pancerella, 2013) and several interpretations of
89 prototypical predator-prey models (Smith, 1991; Hiebeler, 1994; Wilensky, 1997; Tatara et al., 2006;
90 Ottino-Loffler et al., 2007; Ginovart, 2014). Nonetheless, there is a lack of formalization and in-depth sta-
91 tistical analysis of simulation output in most of these implementations, often leading to model assessment
92 and replication difficulties (Edmonds and Hales, 2003; Wilensky and Rand, 2007). This might not come
93 as a surprise, as most models are not implemented with replication in mind.

94 Many models are not adequately analyzed with respect to their output data, often due to improper
95 design of simulation experiments. Consequently, authors of such models can be at risk of making
96 incorrect inferences about the system being studied (Law, 2007). A number of papers and books have
97 been published concerning the challenges, pitfalls and opportunities of using simulation models and
98 adequately analyzing simulation output data. In one of the earliest articles on the subject, Sargent (1976)
99 demonstrates how to obtain point estimates and confidence intervals for steady state means of simulation
100 output data using a number of different methodologies. Later, Law (1983) presented a state-of-the-art
101 survey on statistical analyses for simulation output data, addressing issues such as start-up bias and
102 determination of estimator accuracy. This survey was updated several times over the years, e.g. (Law,
103 2007), where Law discusses the duration of transient periods before steady state settles, as well as the
104 number of replications required for achieving a specific level of estimator confidence. In (Kelton, 1997),
105 the author describes methods to help design the runs for simulation models and interpreting their output
106 using statistical methods, also dealing with related problems such as model comparison, variance reduction
107 or sensitivity estimation. A comprehensive exposition of these and other important topics of simulation
108 research is presented in the several editions of "Simulation Modeling and Analysis" by Law and Kelton,
109 and its latest edition (Law, 2015) is used as a starting point for the analysis described in 'Methodology'
110 and conducted in 'Results'.

111 METHODOLOGY

112 Overview, design concepts and details of PPHPC

113 Here we describe the PPHPC model using the ODD protocol (Grimm et al., 2010). Time-dependent state
114 variables are represented with uppercase letters, while constant state variables and parameters are denoted
115 by lowercase letters. The $U(a, b)$ expression equates to a random integer within the closed interval $[a, b]$
116 taken from the uniform distribution.

117 Purpose

118 The purpose of PPHPC is to serve as a standard model for studying and evaluating SABM implementation
119 strategies. It is a realization of a predator-prey dynamic system, and captures important characteristics
120 of SABMs, such as agent movement and local agent interactions. The model can be implemented using
121 substantially different approaches that ensure statistically equivalent qualitative results. Implementations
122 may differ in aspects such as the selected system architecture, choice of programming language and/or
123 agent-based modeling framework, parallelization strategy, random number generator, and so forth. By
124 comparing distinct PPHPC implementations, valuable insights can be obtained on the computational and
125 algorithmical design of SABMs in general.

126 Entities, state variables, scales

127 The PPHPC model is composed of three entity classes: *agents*, *grid cells* and *environment*. Each of these
128 entity classes is defined by a set of state variables, as shown in Table 1. All state variables explicitly assume
129 integer values to avoid issues with the handling of floating-point arithmetic on different programming
130 languages and/or processor architectures.

131 The t state variable defines the *agent* type, either s (*sheep*, i.e. prey) or w (*wolf*, i.e. predator). The
132 only behavioral difference between the two types is in the feeding pattern: while prey consume passive
133 cell-bound food, predators consume prey. Other than that, prey and predators may have different values
134 for other state variables, as denoted by the superscripts s and w . Agents have an energy state variable,
135 E , which increases by g^s or g^w when feeding, decreases by l^s or l^w when moving, and decreases by half
136 when reproducing. When energy reaches zero, the agent is removed from the simulation. Agents with
137 energy higher than r_T^s or r_T^w may reproduce with probability given by r_p^s or r_p^w . The grid position state
138 variables, X and Y , indicate which cell the agent is located in. There is no conceptual limit on the number
139 of agents that can exist during the course of a simulation run.

Entity	State variable	Symbol	Range
Agents	Type	t	w, s
	Energy	E	$1, 2, \dots$
	Horizontal position in grid	X	$0, 1, \dots, x_{\text{env}} - 1$
	Vertical position in grid	Y	$0, 1, \dots, y_{\text{env}} - 1$
	Energy gain from food	g^s, g^w	$0, 1, \dots$
	Energy loss per turn	l^s, l^w	$0, 1, \dots$
	Reproduction threshold	r_T^s, r_T^w	$1, 2, \dots$
	Reproduction probability	r_P^s, r_P^w	$0, 1, \dots, 100$
Grid cells	Horizontal position in grid	x	$0, 1, \dots, x_{\text{env}} - 1$
	Vertical position in grid	y	$0, 1, \dots, y_{\text{env}} - 1$
	Countdown	C	$0, 1, \dots, c_r$
Environment	Horizontal size	x_{env}	$1, 2, \dots$
	Vertical size	y_{env}	$1, 2, \dots$
	Restart	c_r	$1, 2, \dots$

Table 1. Model state variables by entity. Where applicable, the s and w designations correspond to prey (*sheep*) and predator (*wolf*) agent types, respectively.

140 Instances of the *grid cell* entity class can be thought of the place or neighborhood where agents act,
 141 namely where they try to feed and reproduce. Agents can only interact with other agents and resources
 142 located in the same grid cell. Grid cells have a fixed grid position, (x, y) , and contain only one resource,
 143 cell-bound food (*grass*), which can be consumed by prey, and is represented by the countdown
 144 variable C . The C state variable specifies the number of iterations left for the cell-bound food to become
 145 available. Food becomes available when $C = 0$, and when a prey consumes it, C is set to c_r .

146 The set of all grid cells forms the *environment* entity, a toroidal square grid where the simulation takes
 147 place. The environment is defined by its size, $(x_{\text{env}}, y_{\text{env}})$, and by the restart parameter, c_r .

148 Spatial extent is represented by the aforementioned square grid, of size $(x_{\text{env}}, y_{\text{env}})$, where x_{env} and
 149 y_{env} are positive integers. Temporal extent is represented by a positive integer m , which represents the
 150 number of discrete simulation steps or iterations. Spatial and temporal scales are merely virtual, i.e. they
 151 do not represent any real measure.

152 **Process overview and scheduling**

153 Algorithm 1 describes the simulation schedule and its associated processes. Execution starts with an
 154 initialization process, $\text{Init}()$, where a predetermined number of agents are randomly placed in the
 155 simulation environment. Cell-bound food is also initialized at this stage.

156 After initialization, and to get the simulation state at iteration zero, outputs are gathered by the
 157 $\text{GetStats}()$ process. The scheduler then enters the main simulation loop, where each iteration is
 158 sub-divided into four steps: 1) agent movement ; 2) food growth in grid cells ; 3) agent actions ; and, 4)
 159 gathering of simulation outputs.

160 State variables are asynchronously updated, i.e. they are assigned a new value as soon as this value is
 161 calculated by a process (e.g. when an agent gains energy by feeding).

162 **Design concepts**

163 **Basic principles** The general concepts of this model are based on well studied predator-prey dynamics,
 164 initially through analytical approaches (Lotka, 1925; Volterra, 1926), and later using agent-based models
 165 (Smith, 1991). However, PPHPC is designed so that it can be correctly implemented using diverse
 166 computational approaches. Realizations of this model can provide valuable information on how to better
 167 implement SABMs on different computing architectures, namely parallel ones. In particular, they may
 168 shown the impact of different parallelization strategies on simulation performance.

169 **Emergence** The model is characterized by oscillations in the population of both prey and predator,
 170 as well as in the available quantity of cell-bound food. Typically, a peak of predator population occurs
 171 slightly after a peak in prey population size, while quantity of cell-bound food is approximately in “phase

Algorithm 1 Main simulation algorithm. **for** loops can be processed in *any order* or in *random order*. In terms of expected dynamic behavior, the former means the order is not relevant, while the latter specifies loop iterations should be explicitly shuffled.

```

1: INIT()
2: GETSTATS()
3:  $i \leftarrow 1$ 
4: for  $i \leq m$  do
5:   for each agent do                                     ▷ Any order
6:     MOVE()
7:   end for
8:   for each grid cell do                                 ▷ Any order
9:     GROWFOOD()
10:  end for
11:  for each agent do                                     ▷ Random order
12:    ACT()
13:  end for
14:  GETSTATS()
15:   $i \leftarrow i + 1$ 
16: end for

```

172 opposition” with the prey’s population size.

173 **Sensing** Agents can sense the presence of food in the grid cell in which they are currently located. This
 174 means different thing for prey and predators. Prey agents can read the local grid cell C state variable,
 175 which if zero, means there is food available. Predator agents can determine the presence of prey agents.

176 **Interaction** Agents interact with sources of food present in the grid cell they are located in.

177 **Stochasticity** The following processes are random: a) initialization of specific state variables ; b) agent
 178 movement ; c) the order in which agents act ; and, d) agent reproduction.

179 **Observation** The following vector is collected in the `GetStats()` process, where i refers to the
 180 current iteration:

$$\mathbf{O}_i = (P_i^s, P_i^w, P_i^c, \bar{E}_i^s, \bar{E}_i^w, \bar{C}_i)$$

181 P_i^s and P_i^w refer to the total prey and predator population counts, respectively, while P_i^c holds the
 182 quantity of available cell-bound food. \bar{E}_i^s and \bar{E}_i^w contain the mean energy of prey and predator populations.
 183 Finally, \bar{C}_i refers to the mean value of the C state variable in all grid cells.

184 Initialization

185 The initialization process begins by instantiating the *environment* entity, a toroidal square grid, and filling
 186 it with $x_{\text{env}} \times y_{\text{env}}$ grid cells. The initial value of the countdown state variable in each grid cell, C_0 , is set
 187 according to Eq. 1,

$$C_0 = \begin{cases} U(1, c_r), & \text{if } c_0 = 0 \\ 0, & \text{if } c_0 = 1 \end{cases}, \quad \text{with } c_0 = U(0, 1) \quad (1)$$

188 In other words, cell-bound food is initially available with 50% probability. If not available, the
 189 countdown state variable is set to a random value between 1 and c_r .

190 The initial value of the state variables for each agent is determined according to Eqs. 2 and 3.

$$E_0 = U(1, 2g), \quad \text{with } g \in \{g^s, g^w\} \quad (2)$$

$$(X_0, Y_0) = (U(0, x_{\text{env}} - 1), U(0, y_{\text{env}} - 1)) \quad (3)$$

191 **Submodels**

192 As stated in *Process overview and scheduling*, each iteration of the main simulation loop is sub-divided
 193 into four steps, described in the following paragraphs.

194 **Move()** In step 1, agents `Move()`, in any order, within a Von Neumann neighborhood, i.e. up, down,
 195 left, right or stay in the same cell, with equal probability. Agents lose l^s or l^w units of energy when they
 196 move, even if they stay in the same cell; if energy reaches zero, the agent dies and is removed from the
 197 simulation.

198 **GrowFood()** In step 2, during the `GrowFood()` process, each grid cell checks if $C = 0$ (meaning there
 199 is food available). If $C > 0$ it is decremented by one unit. Eq. 4 summarizes this process.

$$C_i = \max(C_{i-1} - 1, 0) \quad (4)$$

200 **Act()** In step 3, agents `Act()` in explicitly random order, i.e. the agent list should be shuffled before
 201 the agents have a chance to act. The `Act()` process is composed of two sub-actions: `TryEat()`
 202 and `TryReproduce()`. The `Act()` process is atomic, i.e. once called, both `TryEat()` and
 203 `TryReproduce()` must be performed; this implies that prey agents may be killed by predators before
 204 or after they have a chance of calling `Act()`, but not during the call.

205 **TryEat()** Agents can only interact with sources of food present in the grid cell they are located in.
 206 Predator agents can kill and consume prey agents, removing them from the simulation. Prey agents can
 207 consume cell-bound food, resetting the local grid cell C state variable to c_r . A predator can consume one
 208 prey per iteration, and a prey can only be consumed by one predator. Agents who act first claim the food
 209 resources available in the local grid cell. Feeding is automatic: if the resource is there and no other agent
 210 has yet claimed it, the agent will consume it. Moreover, only one prey can consume the local cell-bound
 211 food if available (i.e. if $C = 0$). When an agent successfully feeds, its energy E is incremented by g^s or
 212 g^w , depending on whether the agent is a prey or a predator, respectively.

213 **TryReproduce()** If the agent's energy, E , is above its species reproduction threshold, r_T^s or r_T^w , then
 214 reproduction will occur with probability given by the species reproduction probability, r_p^s or r_p^w , as shown
 215 in Algorithm 2. When an agent successfully reproduces, its energy is divided (using integer division)
 216 with its offspring. The offspring is placed in the same grid cell as his parent, but can only take part in the
 217 simulation in the next iteration. More specifically, newly born agents cannot `Act()`, nor be acted upon.
 218 The latter implies that newly born prey cannot be consumed by predators in the current iteration. Agents
 219 immediately update their energy if they successfully feed and/or reproduce.

Algorithm 2 Agent reproduction.

```

function TRYREPRODUCE()
  if  $E > r_T$  then
    if  $U(0, 99) < r_p$  then
       $E^{\text{child}} \leftarrow E/2$  ▷ Integer division
       $E \leftarrow E - E^{\text{child}}$ 
      NEWAGENT( $t, E^{\text{child}}, X, Y$ )
    end if
  end if
end function
  
```

220 **Parameterization** Model parameters can be qualitatively separated into size-related and dynamics-
 221 related parameters, as shown in Table 2. Although size-related parameters also influence model dynamics,
 222 this separation is useful for parameterizing simulations.

223 Concerning size-related parameters, more specifically, the grid size, we propose a base value of
 224 100×100 , associated with 400 prey and 200 predators. Different grid sizes should have proportionally
 225 assigned agent population sizes, as shown in Table 3. In other words, there are no changes in the agent
 226 density nor the ratio between prey and predators.

Type	Parameter	Symbol
Size	Environment size	x_{env}, y_{env}
	Initial agent count	P_0^s, P_0^w
	Number of iterations	m
Dynamics	Energy gain from food	g^s, g^w
	Energy loss per turn	l^s, l^w
	Reproduction threshold	r_T^s, r_T^w
	Reproduction probability	r_P^s, r_P^w
	Cell food restart	c_r

Table 2. Size-related and dynamics-related model parameters.

Size	$x_{env} \times y_{env}$	P_0^s	P_0^w
100	100 × 100	400	200
200	200 × 200	1600	800
400	400 × 400	6400	3200
800	800 × 800	25 600	12 800
1600	1600 × 1600	102 400	51 200
⋮	⋮	⋮	⋮

Table 3. A selection of initial model sizes.

227 For the dynamics-related parameters, we propose two sets of parameters, Table 4, which generate
 228 two distinct dynamics. The second parameter set typically yields more than twice the number of agents
 229 than the first parameter set. Matching results with runs based on distinct parameters is necessary in order
 230 to have a high degree of confidence in the similarity of different implementations (Edmonds and Hales,
 231 2003). While many more combinations of parameters can be experimented with this model, these two
 232 sets are the basis for testing and comparing PPHPC implementations. We will refer to a combination of
 233 model size and parameter set as “size@set”, e.g. 400@1 for model size 400, parameter set 1.

Parameter	Symbol	Set 1	Set 2
Prey energy gain from food	g^s	4	30
Prey energy loss p/ turn	l^s	1	1
Prey reprod. threshold	r_T^s	2	2
Prey reprod. probability	r_P^s	4	10
Predator energy gain from food	g^w	20	10
Predator energy loss p/ turn	l^w	1	1
Predator reprod. threshold	r_T^w	2	2
Predator reprod. probability	r_P^w	5	5
Cell food restart	c_r	10	15

Table 4. Dynamics-related parameter sets.

234 While simulations of the PPHPC model are essentially non-terminating¹, the number of iterations, m ,
 235 is set to 4000, as it allows to analyze steady-state behavior for all the parameter combinations discussed
 236 here.

237 A NetLogo implementation

238 NetLogo is a well-documented programming language and modeling environment for ABMs, focused on
 239 both research and education. It is written in Scala and Java and runs on the Java Virtual Machine (JVM). It

¹A non-terminating simulation is one for which there is no natural event to specify the length of a run (Law, 2015).

240 uses a hybrid interpreter and compiler that partially compiles ABM code to JVM bytecode (Sondahl et al.,
 241 2006). It comes with powerful built-in procedures and is relatively easy to learn, making ABMs more
 242 accessible to researchers without programming experience (Martin et al., 2012). Advantages of having
 243 a NetLogo version include real-time visualization of simulation, pseudo-code like model descriptions,
 244 simplicity in changing and testing different model aspects and parameters, and command-line access for
 245 batch runs and cycling through different parameter sets, even allowing for multithreaded simultaneous
 246 execution of multiple runs. A NetLogo reference implementation is also particularly important as a point
 247 of comparison with other ABM platforms (Isaac, 2011).

248 The NetLogo implementation of PPHPC, Figure 1, is based on NetLogo's own *Wolf Sheep Predation*
 249 model (Wilensky, 1997), considerably modified to follow the ODD discussed in the previous section.
 250 Most NetLogo models will have at least a *setup* procedure, to set up the initial state of the simulation, and
 251 a *go* procedure to make the model run continuously (Wilensky, 2014). The *Init()* and *GetStats()*
 252 processes (lines 1 and 2 of algorithm 1) are defined in the *setup* procedure, while the main simulation
 253 loop is implemented in the *go* procedure. The latter has an almost one-to-one relation with its pseudo-
 254 code counterpart in Algorithm 1. By default, NetLogo shuffles agents before issuing them orders,
 255 which fits naturally into the model ODD. The implementation is available at [https://github.com/
 256 FakenMC/pphc/tree/netlogo](https://github.com/FakenMC/pphc/tree/netlogo).

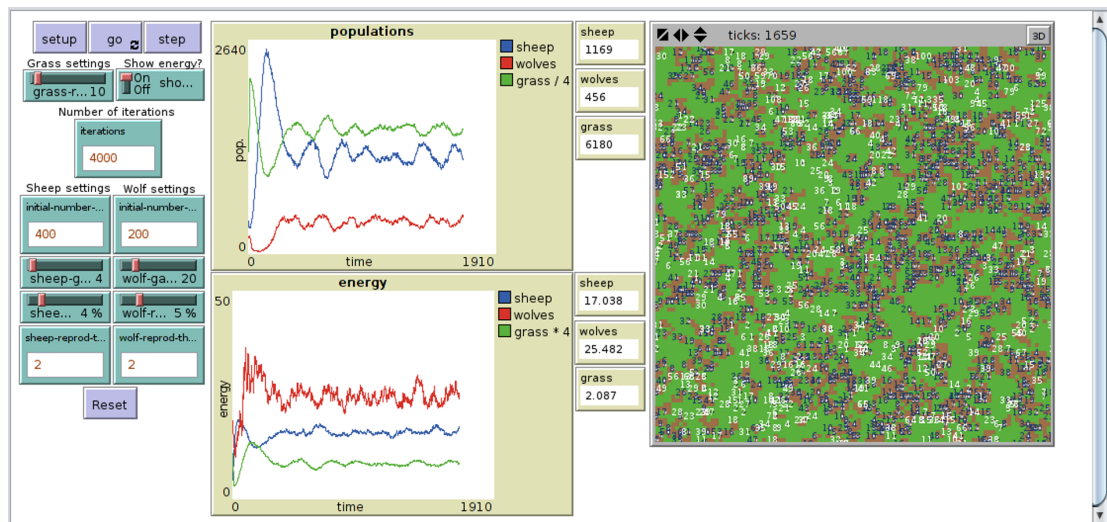


Figure 1. NetLogo implementation of the PPHPC model.

257 Selection of focal measures

258 In order to analyze the output of a simulation model from a statistical point-of-view, we should first
 259 select a set of focal measures (f.m.'s) which summarize each output. Wilensky and Rand (2007) use
 260 this approach in the context of statistical comparison of replicated models. Typically, f.m.'s consist of
 261 long-term or steady-state means. However, being limited to analyze average system behavior can lead to
 262 incorrect conclusions (Law, 2015). Consequently, other measures such as proportions or extreme values
 263 can be used to assess model behavior. In any case, the selection of f.m.'s is an empirical exercise and is
 264 always dependent of the model under study. A few initial runs are usually required in order to perform
 265 this selection.

266 For the PPHPC model, the typical output of a simulation run is shown in Figure 2 for size 400 and
 267 both parameter sets. In both cases, all outputs undergo a transient stage and tend to stabilize after a certain
 268 number of iterations, entering steady-state. For other sizes, the situation is similar apart from a vertical
 269 scaling factor. Outputs display pronounced extreme values in the transient stage, while circling around a
 270 long-term mean and approximately constant standard deviation in the steady-state phase. This standard
 271 deviation is an important feature of the outputs, as it marks the overall variability of the predator-prey
 272 cycles. Having this under consideration, six statistics, described in Table 5, were selected for each output.
 273 Considering there are six outputs, a total of 36 f.m.'s are analyzed for the PPHPC model.

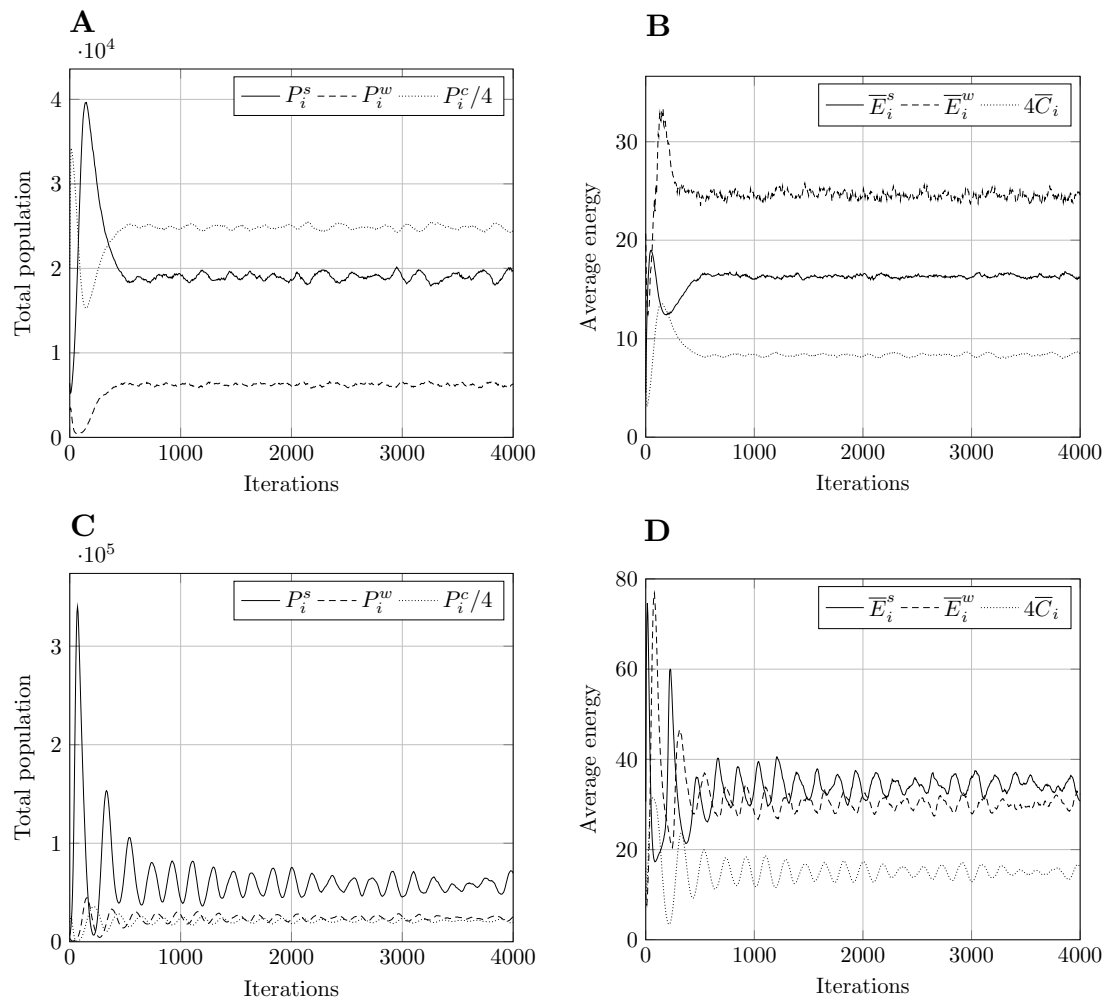


Figure 2. Typical model output for model size 400. Other model sizes have outputs which are similar, apart from a vertical scaling factor. P_i refers to total population, \bar{E}_i to mean energy and \bar{C}_i to mean value of the countdown state variable, C . Superscript s relates to prey, w to predators, and c to cell-bound food. P_i^c and \bar{C}_i are scaled for presentation purposes. (A) Population, param. set 1. (B) Energy, param. set 1. (C) Population, param. set 2. (D) Energy, param. set 2.

274 Collecting and preparing data for statistical analysis

275 Let $X_{j0}, X_{j1}, X_{j2}, \dots, X_{jm}$ be an output from the j^{th} simulation run (rows under 'Iterations' in Table 6). The
 276 X_{ji} 's are random variables that will, in general, be neither independent nor identically distributed (Law,
 277 2015), and as such, are not adequate to be used directly in many formulas from classical statistics (which
 278 are discussed in the next section). On the other hand, let $X_{1i}, X_{2i}, \dots, X_{ni}$ be the observations of an output at
 279 iteration i for n runs (columns under 'Iterations' in Table 6), where each run begins with the same initial
 280 conditions but uses a different stream of random numbers as a source of stochasticity. The X_{ji} 's will now
 281 be independent and identically distributed (i.i.d.) random variables, to which classical statistical analysis
 282 can be applied. However, individual values of the output X at some iteration i are not representative of X
 283 as a whole. Thus, we use the selected f.m.'s as representative summaries of an output, as shown in Table 6,
 284 under 'Focal measures'. Taken column-wise, the observations of the f.m.'s are i.i.d. (because they are
 285 obtained from i.i.d. replications), constituting a *sample* prone to statistical analysis.

286 Regarding steady-state measures, \bar{X}^{ss} and S^{ss} , care must be taken with initialization bias, which may
 287 cause substantial overestimation or underestimation of the long-term performance (Sanchez, 1999). Such
 288 problems can be avoided by discarding data obtained during the initial transient period, before the system
 289 reaches steady-state conditions. The simplest way of achieving this is to use a fixed truncation point, l , for

Statistic	Description
$\max_{0 \leq i \leq m} X_i$	Maximum value.
$\arg \max_{0 \leq i \leq m} X_i$	Iteration where maximum value occurs.
$\min_{0 \leq i \leq m} X_i$	Minimum value.
$\arg \min_{0 \leq i \leq m} X_i$	Iteration where minimum value occurs.
$\bar{X}^{ss} = \sum_{i=l+1}^m X_i / (m-l)$	Steady-state mean.
$S^{ss} = \sqrt{\frac{\sum_{i=l+1}^m (X_i - \bar{X}^{ss})^2}{m-l-1}}$	Steady-state sample standard deviation.

Table 5. Statistical summaries for each output X , where X_i is the value of X at iteration i , m denotes the last iteration, and l corresponds to the iteration separating the transient and steady-state stages.

Rep.	Iterations					Focal measures					
1	X_{10}	X_{11}	...	$X_{1,m-1}$	$X_{1,m}$	$\max X_1$	$\arg \max X_1$	$\min X_1$	$\arg \min X_1$	\bar{X}_1^{ss}	S_1^{ss}
2	X_{20}	X_{21}	...	$X_{2,m-1}$	$X_{2,m}$	$\max X_2$	$\arg \max X_2$	$\min X_2$	$\arg \min X_2$	\bar{X}_2^{ss}	S_2^{ss}
	\vdots	\vdots		\vdots	\vdots	\vdots	\vdots	\vdots	\vdots	\vdots	\vdots
n	X_{n0}	X_{n1}	...	$X_{n,m-1}$	$X_{n,m}$	$\max X_n$	$\arg \max X_n$	$\min X_n$	$\arg \min X_n$	\bar{X}_n^{ss}	S_n^{ss}

Table 6. Values of a generic simulation output (under ‘Iterations’) for n replications of m iterations each (plus iteration 0, i.e. the initial state), and the respective f.m.’s (under ‘Focal measures’). Values along columns are i.i.d..

290 all runs with the same initial conditions, selected such that: a) it systematically occurs after the transient
 291 state; and, b) it is associated with a round and clear value, which is easier to communicate (Sanchez, 1999).
 292 Law (2015) suggests the use of Welch’s procedure (Welch, 1981) in order to empirically determine l . Let
 293 $\bar{X}_0, \bar{X}_1, \bar{X}_2, \dots, \bar{X}_m$ be the averaged process taken column-wise from Table 6 (columns under ‘Iterations’),
 294 such that $\bar{X}_i = \sum_{j=1}^n X_{ji} / n$ for $i = 0, 1, \dots, m$. The averaged process has the same transient mean curve as
 295 the original process, but its variance is reduced by a factor of n . A low-pass filter can be used to remove
 296 short-term fluctuations, leaving the long-term trend of interest, allowing us to visually determine a value
 297 of l for which the averaged process seems to have converged. A moving average approach can be used for
 298 filtering:

$$\bar{X}_i(w) = \begin{cases} \frac{\sum_{s=-w}^w \bar{X}_{i+s}}{2w+1} & \text{if } i = w+1, \dots, m-w \\ \frac{\sum_{s=-(i-1)}^{i-1} \bar{X}_{i+s}}{2i-1} & \text{if } i = 1, \dots, w \end{cases} \quad (5)$$

299 where w , the *window*, is a positive integer such that $w \leq \lfloor m/4 \rfloor$. This value should be large enough
 300 such that the plot of $\bar{X}_i(w)$ is moderately smooth, but not any larger. A more in-depth discussion of this
 301 procedure is available in (Welch, 1981; Law, 2015).

302 Statistical analysis of focal measures

303 Let Y_1, Y_2, \dots, Y_n be i.i.d. observations of some f.m. with finite population mean μ and finite population
 304 variance σ^2 (i.e. any column under ‘Focal measures’ in Table 6). Then, as described by Law (2007, 2015),
 305 unbiased point estimators for μ and σ^2 are given by

$$\bar{Y}(n) = \frac{\sum_{j=1}^n Y_j}{n} \quad (6)$$

306 and

$$S^2(n) = \frac{\sum_{j=1}^n [Y_j - \bar{Y}(n)]^2}{n-1} \quad (7)$$

307 respectively.

308 Another common statistic usually determined for a given f.m. is the confidence interval (c.i.) for $\bar{Y}(n)$,
 309 which can be defined in several different ways. The t -distribution c.i. is commonly used for this purpose
 310 (Law, 2007, 2015), although it has best coverage for normally distributed samples, which is often not the
 311 case for simulation models in general (Sargent, 1976; Law, 2015) and agent-based models in particular
 312 (Helbing and Balmelli, 2012). If samples are drawn from populations with multimodal, discrete or strongly
 313 skewed distributions, the usefulness of t -distribution c.i.'s is further reduced. While there is not much to
 314 do in the case of multimodal distributions, Law (2015) proposes the use of the c.i. developed by Willink
 315 (2005), which takes distribution skewness into account. Furthermore, c.i.'s for discrete distributions
 316 are less studied and usually assume data follows a binomial distribution, presenting some issues of its
 317 own (Brown et al., 2001). As suggested by Radax and Rengs (2010), we focus on providing a detailed
 318 assessment of the distributional properties of the different f.m.'s, namely whether they are sufficiently
 319 "normal" such that normality-assuming (parametric) statistical techniques can be applied, not only for c.i.
 320 estimation, but also for model comparison purposes.

321 The normality of a data set can be assessed graphically or numerically (Park, 2008). The former
 322 approach is intuitive, lending itself to empirical interpretation by providing a way to visualize how random
 323 variables are distributed. The latter approach is a more objective and quantitative form of assessing
 324 normality, providing summary statistics and/or statistics tests of normality. In both approaches, specific
 325 methods can be either descriptive or theory-driven, as shown in Table 7.

	Graphical methods	Numerical methods
Descriptive	Histogram , Box plot, Dot plot	Skewness , Kurtosis
Theory-driven	Q-Q plot , P-P plot	Shapiro-Wilk , Anderson-Darling, Cramer-von Mises, Kolmogorov- Smirnov, Jarque-Bera and other tests

Table 7. Methods for assessing the normality of a data set, adapted from Park (2008). Boldface methods are used in this study.

326 For this study we chose one method of each type, as shown in boldface in Table 7. This approach not
 327 only provides a broad overview of the distribution under study, but is also important because no single
 328 method can provide a complete picture of the distribution.

329 Under the graphical methods umbrella, a **histogram** shows the approximate distribution of a data set,
 330 and is built by dividing the range of values into a sequence of intervals (*bins*), and counting how many
 331 values fall in each interval. A **Q-Q plot** compares the distribution of a data set with a specific theoretical
 332 distribution (e.g., the normal distribution) by plotting their quantiles against each other (thus "Q-Q").
 333 If the two distributions match, the points on the plot will approximately lie on the $y = x$ line. While a
 334 histogram gives an approximate idea of the overall distribution, the Q-Q plot is more adequate to see how
 335 well a theoretical distribution fits the data set.

336 Concerning numerical methods, **Skewness** measures the degree of symmetry of a probability distribu-
 337 tion about its mean, and is a commonly used metric in the analysis of simulation output data (Sargent,
 338 1976; Nakayama, 2008; Law, 2015). If skewness is positive, the distribution is skewed to the right, and if
 339 negative, the distribution is skewed to the left. Symmetric distributions have zero skewness, however, the
 340 converse is not necessarily true, e.g. skewness will also be zero if both tails of an asymmetric distribution
 341 account for half the total area underneath the probability density function. In the case of theory-driven
 342 numerical approaches, we select the **Shapiro-Wilk** (SW) test (Shapiro and Wilk, 1965), as it has been
 343 shown to be more effective when compared to several other normality tests (Razali and Wah, 2011). We
 344 focus on the p -value of this test (instead of the test's own W statistic), as it is an easily interpretable

345 measure. The null-hypothesis of this test is that the data set, or sample, was obtained from a normally
346 distributed population. If the p -value is greater than a predetermined significance level α , usually 0.01 or
347 0.05, then the null hypothesis cannot be rejected. Conversely, a p -value less than α implies the rejection
348 of the null hypothesis, i.e. that the sample was not obtained from a normally distributed population.

349 RESULTS

350 A total of 30 replications, $r = 1, \dots, 30$, were performed with NetLogo 5.1.0 for each combination of
351 model sizes (Table 3) and parameters sets (Table 4). Each replication r was performed with a PRNG seed
352 obtained by taking the MD5 checksum of r and converting the resulting hexadecimal string to a 32-bit
353 integer (the maximum precision accepted by NetLogo), guaranteeing some independence between seeds,
354 and consequently, between replications. The list of seeds is provided in Table S1.

355 Determining the steady-state truncation point

356 Using Welch's method, we smoothed the averaged outputs using a moving average filter with $w = 10$.
357 Having experimented with other values, $w = 10$ seemed to be a good compromise between rough and
358 overly smooth plots. Figure 3 shows results for model size 400 and both parameter sets. Following the
359 recommendations described in section 'Methodology', we select the steady-state truncation point to be
360 $l = 1000$ for parameter set 1, and $l = 2000$ for parameter set 2. These are round values which appear to
361 occur after the transient stage. Other model sizes produce similar results, apart from a vertical scaling
362 factor, which means that these values of l are also applicable in those cases.

363 Analyzing the distributions of focal measures

364 The six statistic summaries for each f.m., namely mean, sample variance, p -value of the SW test, skewness,
365 histogram and Q-Q plot, are shown in Tables S2.1 to S2.10 (available as supplemental information) for all
366 model size and parameter set combinations. The number of bins in the histograms is set to the minimum
367 between 10 (an appropriate value for a sample size of 30) and the number of unique values in the data set.

368 Much of the information provided in Tables S2.1 to S2.10, namely the p -value of the SW test, the
369 skewness, and the Q-Q plots, is geared towards continuous distributions. However, f.m.'s taken from *arg*
370 *max* and *arg min* operators only yield integer (discrete) values, which correspond to specific iterations. The
371 same is true for *max* and *min* of population outputs, namely P_i^s , P_i^w , and P_i^c . This can be problematic for
372 statistic summaries taken from integer-valued f.m.'s with a small number of unique values. For example,
373 the SW test will not be very informative in such cases, and cannot even be performed if all observations
374 yield the same value (e.g. *arg max* of P_i^c for 800@1, Table S2.4). Nonetheless, distributional properties of
375 a f.m. can dramatically change for different model size and parameter set combinations. For example,
376 for parameter set 2, observations of the *arg max* of P_i^c span many different values for model size 200
377 (Table S2.7), while for size 1600 (Table S2.10) they are limited to only three different values. Summary
378 statistics appropriate for continuous distributions could be used in the former case, but do not provide
379 overly useful information in the latter. In order to maintain a consistent approach, our discussion will
380 continue mainly from a continuous distribution perspective, more specifically by analyzing how closely
381 a given f.m. follows the normal distribution, though we superficially examine its discrete nature when
382 relevant.

383 Distribution of focal measures over the several size@set combinations

384 In the next paragraphs we describe the distributional behavior of each f.m., and when useful, repeat in a
385 compact fashion some of the information provided in Tables S2.1 to S2.10.

386 $\max P_i^s$: The SW p -value is consistently above the 5% significance level, skewness is usually low and
387 with an undefined trend, and the Q-Q plots are mostly follow the $y = x$ line. Although there are borderline
388 cases, such as 800@1 and 1600@2, the summary statistics show that the maximum prey population f.m.
389 generally follows an approximately normal distribution.

390 $\arg \max P_i^s$: This f.m. follows an approximately normal distribution for smaller sizes of parameter set 1,
391 but as model size grows larger, the discrete nature of the data clearly stands out. This behavior is more
392 pronounced for parameter set 2 (which yields simulations inherently larger than parameter set 1), such
393 that, for 1600@2, all observations yield the same value (i.e. 70). Table 8 shows, using histograms, how
394 the distribution qualitatively evolves over the several size@set combinations.

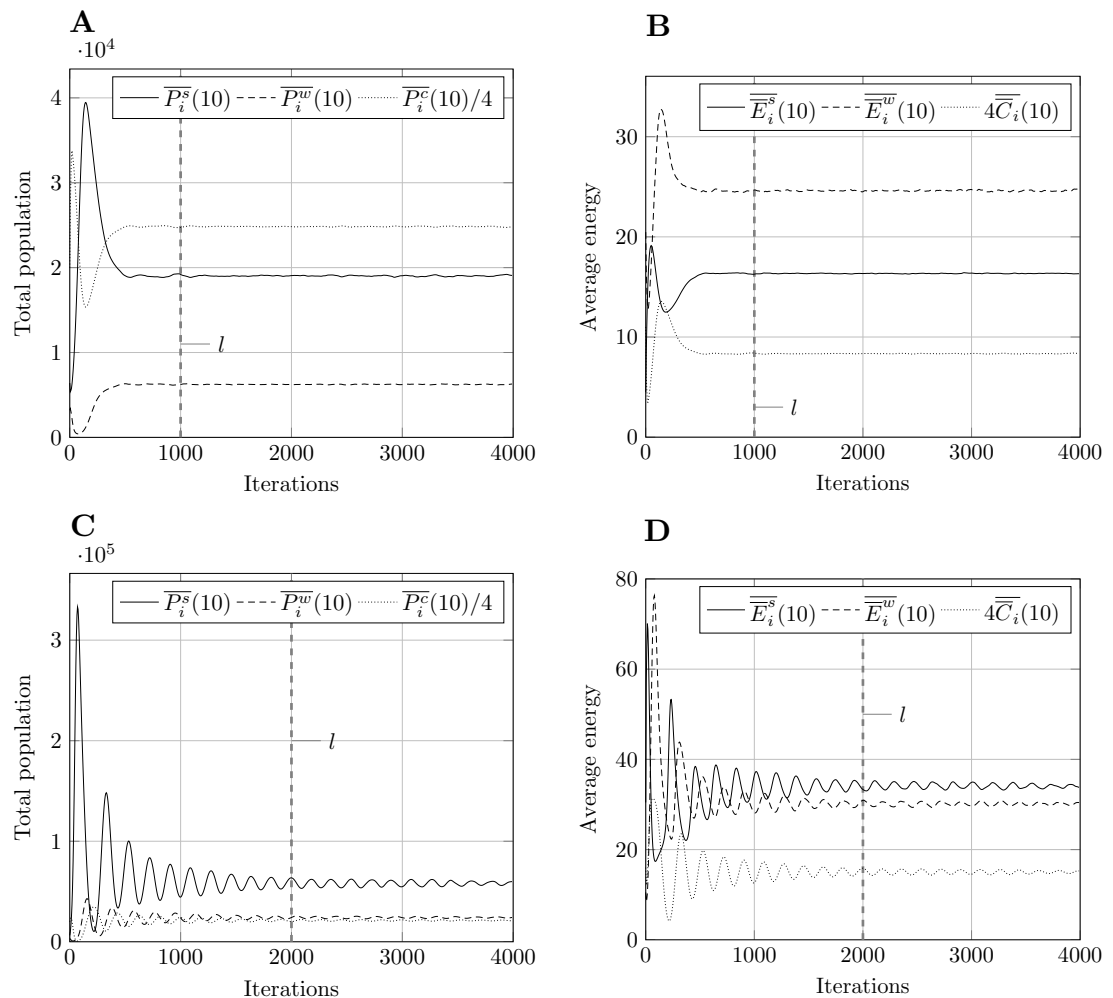


Figure 3. Moving average of outputs for model size 400 with $w = 10$. Other model sizes produce similar results, apart from a vertical scaling factor. The dashed vertical line corresponds to iteration l after which the output is considered to be in steady-state. (A) Population moving average, param. set 1. (B) Energy moving average, param. set 1. (C) Population moving average, param. set 2. (D) Energy moving average, param. set 2.

395 $\min P_i^{ss}$: Two very different behaviors are observed for the two parameter sets. In the case of parameter set
 396 1, this f.m. has a slightly negatively skewed distribution, with some p -values below the 0.05 significance
 397 threshold, but is otherwise not very far from normality (this is quite visible in some histograms). However,
 398 for parameter set 2, the data is more concentrated on a single value, more so for larger sizes. Note that
 399 this single value is the initial number of prey, which means that, in most cases, the minimum number of
 400 prey never drops below its initial value.

401 $\arg \min P_i^{ss}$: This f.m. follows a similar pattern to the previous one, but more pronounced in terms of
 402 discreteness, namely for parameter set 1. For parameter set 2, sizes 100 and 200, the distribution is
 403 bimodal, with the minimum prey population occurring at iteration zero (i.e. initial state) or around
 404 iteration 200, while for larger sizes, the minimum always occurs at iteration zero.

405 \bar{P}_i^{ss} : The prey population steady-state mean seems to generally follow a normal distribution, the only
 406 exception being 400@2, in which some departure from normality is observed, as denoted by a SW p -value
 407 below 0.05 and a few outliers in the Q-Q plot.

408 $S^{ss}(P_i^{ss})$: For most size@set combinations this f.m. does not present large departures from normality.
 409 However, skewness is always positive.

Set \ Size	100	200	400	800	1600
1					
2					

Table 8. Histograms for the several size@set combinations of the $\arg \max P_i^S$ f.m..

410 $\max P_i^w$: This f.m. presents distributions which are either considerably skewed or relatively normal. The
 411 former tend to occur for smaller model sizes, while the latter for larger sizes, although this trend is not
 412 totally clear. The 800@2 sample is a notable case, as it closely follows a normal distribution, with a
 413 symmetric histogram, approximately linear Q-Q plot, and a SW p -value of 0.987.

414 $\arg \max P_i^w$: Interestingly, for parameter set 1, this f.m. seems to follow a uniform distribution. This
 415 is more or less visible in the histograms, but also in the Q-Q plots, because when we plot uniform data
 416 points against a theoretical normal distribution in a Q-Q plot we get the “stretched-S” pattern which is
 417 visible in this case (Table 9). For parameter set 2, the distribution seems to be more normal, or even
 418 binomial as the discreteness of the data starts to stand-out for larger model sizes; the only exception is for
 419 size 100, which presents a multimodal distribution.

Set \ Size	100	200	400	800	1600
1					
2					

Table 9. Q-Q plots for the several size@set combinations of the $\arg \max P_i^w$ f.m..

420 $\min P_i^w$: The minimum predator population seems to follow an approximately normal distribution, albeit
 421 with a slight positive skewness, except for 800@1, which has negative skewness.

422 $\arg \min P_i^w$: This f.m. displays an approximately normal distribution. However, for larger simulations
 423 (i.e. mainly for parameter set 2) the discrete nature of the data becomes more apparent.

424 \overline{P}_i^{wSS} : The steady-state mean of predator population apparently follows a normal distributions. This
 425 is confirmed by all summary statistics, such as the SW p -value, which is above 0.05 for all size@set
 426 combinations.

427 $S^{SS}(P_i^w)$: Departure from normality is not large in most cases (200@2 and 800@2 are exceptions,
 428 although the former due to a single outlier), but the trend of positive skewness is again observed for this
 429 statistic.

430 $\max P_i^c$: The maximum available cell-bound food seems to have a normal distribution, although 400@2
 431 has a few outliers which affect the result of the SW p -value (which, nonetheless, is above 0.05).

432 $\arg \max P_i^c$: The behavior of this f.m. is again quite different between parameter sets. For the first
 433 parameter set, the discrete nature of the underlying distribution stands out, with no more than three unique
 434 values for size 100, down to a single value for larger sizes, always centered around the value 12 (i.e.
 435 the maximum available cell-bound food tends to occur at iteration 12). For the second parameter set,
 436 distribution is almost normal for sizes above 200, centered around iteration 218, although its discreteness
 437 shows for larger sizes, namely for size 1600, which only presents three distinct values. For size 100, most
 438 values fall in iteration 346, although two outliers push the mean up to 369.5.

439 $\min P_i^c$: This f.m. displays an apparently normal distribution for all model sizes and parameter sets, with
 440 the exception of 800@1, which has a few outliers at both tails of the distribution, bringing down the SW
 441 p -value barely above the 5% significance level.

442 $\arg \min P_i^c$: In this case, the trend is similar for both parameter sets, i.e. the distribution seems almost
 443 normal, but for larger sizes the underlying discreteness becomes apparent. This is quite clear for parameter
 444 set 2, as shown in Table 10, where the SW test p -value decreases as the discreteness becomes more visible
 445 in the histograms and Q-Q plots .

Stat. \ Size	100	200	400	800	1600
SW	0.437	0.071	0.062	0.011	< 0.001
Hist.					
Q-Q					

Table 10. Three statistical summaries for the several sizes of the $\arg \min P_i^c$ f.m. for parameter set 2. Row ‘SW’ contains the SW test p -values, while the corresponding histograms and Q-Q plots are in rows ‘Hist.’ and ‘Q-Q’, respectively.

446 \overline{P}_i^{cSS} : For this f.m. there is not a significant departure from normality. The only exception is for 800@1,
 447 but only due to a single outlier.

448 $S^{SS}(P_i^c)$: Like in previous cases, the steady-state sample standard deviation does not stray too far from
 449 normality, but consistently shows a positive skewness.

450 $\max \overline{E}_i^s$: For sizes 100 and 200 of both parameter sets, the maximum of the mean prey energy presents a
 451 positively skewed, lognormal-like distribution. For larger sizes, distributions tend to be more normal-like.
 452 This trend is clear when analyzing how the p -value of the SW test and the skewness vary for the several
 453 size@set combinations, as shown in Table 11, namely for sizes 100 and 200, where the former is smaller
 454 while the absolute value of the latter is larger.

Set	Stat.	Size				
		100	200	400	800	1600
1	SW	0.159	0.012	0.625	0.672	0.555
	Skew.	0.679	0.961	0.521	-0.123	0.196
2	SW	< 0.001	0.038	0.515	0.702	0.337
	Skew.	1.80	1.07	-0.327	-0.216	0.389

Table 11. p -values for the SW test (row ‘SW’) and skewness (row ‘Skew.’) for the several size@set combinations of the $\max \overline{E}_i^s$ f.m..

455 $\arg \max \overline{E}_i^s$: For parameter set 1, the distribution is approximately normal for smaller sizes, with the
 456 underlying discreteness becoming apparent for larger sizes, centering around iteration 49. For parameter
 457 set 2, the data set revolves around a limited set of unique values (centered at iteration 16), following a
 458 poisson-like distribution, except for size 100, which displays a bimodal behavior.

459 $\min \overline{E}_i^s$: This f.m. seems to follow an approximately normal distribution.

460 $\arg \min \overline{E}_i^s$: In the case of parameter set 1, this f.m. has distributions with a single value: zero. This
 461 means that the minimum mean prey energy occurs at the initial state of the simulation. From there
 462 onwards, mean prey energy is always higher. The situation is notably different for the second parameter
 463 set, where minimum mean prey energy can occur at several different iterations centered around iteration
 464 88. Distribution seems to be binomial or Poisson-like.

465 \overline{E}_i^{SS} : Although the histograms are not very clear, the Q-Q plots and the p -values from the SW test
 466 suggest that this f.m. follows a normal distribution.

467 $S^{SS}(\overline{E}_i^s)$: This f.m. does not seem to stray much from normality, except in the case of 1600@1 and 200@2,
 468 which are affected by outliers. The tendency for the steady-state sample standard deviation statistic to
 469 show positive skewness is again confirmed with these observations (800@1 being the exception).

470 $\max \overline{E}_i^w$: The maximum of mean predator energy follows an approximately normal distribution, though
 471 for 100@1 there are a few replications which produce unexpected results.

472 $\arg \max \overline{E}_i^w$: In most cases, this f.m. approximately follows a normal distribution. There are several
 473 exceptions though. For the second parameter set and sizes above 400, the f.m. starts to display its discrete
 474 behavior, following a Poisson-like distribution. Less critically, an outlier “ruins” normality for 100@1.

475 $\min \overline{E}_i^w$: Apart from a few outliers with some parameter combinations, this f.m. generally seems to
 476 follow a normal distribution.

477 $\arg \min \overline{E}_i^w$: Perhaps with the exception of 100@1 and 200@1, the iteration where the minimum of mean
 478 predator energy occurs seems best described with a discrete, Poisson-like distribution.

479 \overline{E}_i^{wSS} : This f.m. generally follows a normal distribution. However, 1600@1 shows a salient second peak
 480 (to the right of the histogram, also visible in the Q-Q plot), affecting the resulting SW p -value, which is
 481 below the 1% significance threshold.

482 $S^{SS}(\overline{E}_i^w)$: This f.m. follows a positively skewed unimodal distribution, in the same line as the steady-state
 483 sample standard deviation of other outputs. Note the outlier in 200@2, also observed for the $S^{SS}(P_i^w)$ f.m.,
 484 which is to be expected as both f.m.’s are related to predator dynamics.

485 $\max \overline{C}_i$: The samples representing the maximum of the mean C state variable are most likely drawn from
 486 a normal distribution. Most histograms are fairly symmetric (which is corroborated by the low skewness
 487 values), the Q-Q plots are generally linear, and the SW p -value never drops below 0.05 significance.

488 $\arg \max \overline{C}_i$: For smaller model sizes this f.m. follows a mostly normal distribution, but as with other
 489 iteration-based f.m.’s, the underlying discreteness of the distribution starts to show at larger model sizes,
 490 especially for the second parameter set.

491 $\min \overline{C}_i$: For most size@set combinations, the minimum of the mean C state variable seems to be
 492 normally distributed. Nonetheless, a number of observations for 400@2 yield unexpected values, making
 493 the respective distribution bimodal and distorting its normality (though the respective SW p -value does
 494 not drop below 0.05).

495 $\arg \min \overline{C}_i$: Like in some previous cases, this f.m. displays different behavior depending on the parameter
 496 set. For the first parameter set, practically all observations have the same value, 10, which means the
 497 minimum of the mean C state variable is obtained at iteration 10. Only model sizes 100 and 200 have
 498 some observations representing iterations 11 and/or 12. Parameter set 2 yields a different dynamic, with
 499 an average iteration of 216 approximately (except for size 100, which has an average iteration of 373.3
 500 due to a few very distant outliers). While sizes 200 and 400 follow an approximately normal distribution,
 501 larger sizes seem to be more fit to be analyzed using discrete distributions such as Poisson or binomial.

502 \overline{C}_i^{SS} : This f.m. follows an approximately normal distribution. While most size/parameter combinations
 503 have a few outliers, only for 800@1 is the existing outlier capable of making the SW test produce a
 504 p -value below the 5% significance threshold.

505 $S^{SS}(\overline{C}_i)$: Although passing the SW normality test (p -value > 0.05) in most cases, we again note the
 506 positive skewness of the steady-state sample standard deviation samples, suggesting that distributions
 507 such as Weibull or Lognormal maybe a better fit.

508 **Statistics-wise distribution trends**

509 Table 12 summarizes the descriptions given in the previous section. It was built by assigning an empirical
 510 classification from 0 to 5 to each f.m. according to how close it follows the normal distribution for the
 511 tested size@set combinations. More specifically, individual classifications were determined by analyzing

512 the information provided in Tables S2.1 to S2.10, prioritizing the SW test result (i.e. if the p -value is
 513 above 0.01 and/or 0.05) and distributional discreteness (observable in the Q-Q plots). This classification
 514 can be used as a guide to whether parametric or non-parametric statistical methods should be used to
 515 further analyze the f.m.'s or to compare f.m.'s of different PPHPC implementations. The last row shows
 516 the average classification of individual outputs for a given statistic, outlining its overall normality.

X_i \ Stat.	$\max_{0 \leq i \leq m} X_i$	$\arg \max_{0 \leq i \leq m} X_i$	$\min_{0 \leq i \leq m} X_i$	$\arg \min_{0 \leq i \leq m} X_i$	\bar{X}^{ss}	S^{ss}
P_i^s	●●●●●	●●○○○	●●●○○	○○○○○	●●●●●	●●●●●
P_i^w	●●●●○	●●○○○	●●●●●	●●●○○	●●●●●	●●●●●
P_i^c	●●●●●	●○○○○	●●●●●	●●●○○	●●●●●	●●●●●
\bar{E}_i^s	●●●●○	●○○○○	●●●●●	●○○○○	●●●●●	●●●●●
\bar{E}_i^w	●●●●●	●●●○○	●●●●●	●○○○○	●●●●●	●●●●○
\bar{C}_i	●●●●●	●●○○○	●●●●●	○○○○○	●●●●●	●●●●●
Stat. wise	●●●●●	●●○○○	●●●●●	●○○○○	●●●●●	●●●●●

Table 12. Empirical classification (from 0 to 5) of each f.m. according to how close it follows the normal distribution for the tested size@set combinations. The last row outlines the overall normality of each statistic.

517 The *max* and *min* statistics yield mostly normal distributions, although care should be taken when the
 518 maximum or minimum systematically converge to the same value, e.g. when they occur at iteration zero.
 519 Nonetheless, parametric methods seem adequate for f.m.'s drawn from these statistics. The same does
 520 not apply to the *arg max* and *arg min* statistics, which show a large variety of distributional behaviors
 521 (including normality in some cases). Thus, these statistics are better handled with non-parametric
 522 techniques. The steady-state mean typically displays distributions very close to normal, probably due
 523 to central-limit-theorem type effects, as described by Law (2007) for mean or average-based f.m.'s.
 524 Consequently, parametric methods will most likely be suitable for this statistic. Finally, f.m.'s based on
 525 the steady-state sample standard deviation display normal-like behavior, albeit with consistently positive
 526 skewness; in fact, they are probably better represented by a Weibull or Lognormal distribution. While
 527 parametric methods may be used for this statistic, results should be interpreted cautiously.

528 DISCUSSION

529 In this paper, the PPHPC model is completely specified, and an exhaustive analysis of the respective
 530 simulation outputs is performed. Regarding the latter, after determining the mean and variance of the
 531 several f.m.'s, we opted to study their distributional properties instead of proceeding with the classical
 532 analysis suggested by simulation output analysis literature (i.e. the establishment of c.i.'s.). This approach
 533 has a number of practical uses. For example, if we were to estimate c.i.'s for f.m.'s drawn from the steady-
 534 state mean, we could use t -distribution c.i.'s with some confidence, as these f.m.'s display an approximately
 535 normal distribution. If we did the same for f.m.'s drawn from the steady-state sample standard deviation,
 536 the Willink (2005) c.i. would be preferable, as it accounts for the skewness displayed by these f.m.'s.
 537 Estimating c.i.'s without a good understanding of the underlying distribution can be misleading, especially
 538 if the distribution is multimodal. The approach taken here is also useful for comparing different PPHPC
 539 implementations. If we were to compare *max* or *min*-based f.m.'s, which seem to follow approximately
 540 normal distributions, parametric tests such as the t -test would most likely produce valid conclusions.
 541 On the other hand, if we compare *arg max* or *arg min*-based f.m.'s, non-parametric tests, such as the
 542 Mann-Whitney U test (Gibbons and Chakraborti, 2011), would be more adequate, as these f.m.'s do not
 543 usually follow a normal distribution.

544 However, the scope of the PPHPC model is significantly broader. For example, in (Fachada et al.,
 545 2015b), PPHPC is reimplemented in Java with several user-selectable parallelization strategies. The goal
 546 is to clarify which are the best parallelization approaches for SABMs in general. A n -sample statistical
 547 test is applied to each f.m., for all implementations and strategies simultaneously, in order to verify that
 548 these do not yield dissimilar results. In (Fachada et al., 2015a), PPHPC is used for presenting a novel

549 model-independent comparison technique which directly uses simulation outputs, bypassing the need of
550 selecting model-specific f.m.'s.

551 The PPHPC model is made available to other researchers via the source code, in addition to the
552 specification presented here. All the data analyzed in this paper is also available as supplemental data.
553 PPHPC can be used as a pure computational model without worrying with aspects like visualization and
554 user interfaces, allowing for direct performance comparison of different implementations.

555 CONCLUSION

556 In this paper, we presented PPHPC, a conceptual model which captures important characteristics of
557 SABMs. The model was comprehensively described using the ODD protocol, a NetLogo canonical
558 implementation was reported, and simulation outputs were thoroughly studied from a statistical perspective
559 for two parameter sets and several model sizes. While many ABMs have been published, proper model
560 description and analysis is lacking in the scientific literature, and thus this paper can be seen as a guideline
561 or methodology to improve model specification and communication in the field. Furthermore, PPHPC
562 aims to be a standard model for research in agent-based modeling and simulation, such as, but not limited
563 to, statistical model comparison techniques, performance comparison of parallel implementations, and
564 testing the influence of different PRNGs on the statistical accuracy of simulation output.

565 REFERENCES

- 566 Axtell, R., Axelrod, R., Epstein, J. M., and Cohen, M. D. (1996). Aligning simulation models: a case
567 study and results. *Comput. Math. Organ. Theory*, 1(2):123–141.
- 568 Bigbee, A., Cioffi-Revilla, C., and Luke, S. (2007). Replication of Sugarscape using MASON. In Terano,
569 T., Kita, H., Deguchi, H., and Kijima, K., editors, *Agent-Based Approaches in Economic and Social
570 Complex Systems IV*, volume 3 of *Springer Series on Agent Based Social Systems*, pages 183–190.
571 Springer Japan.
- 572 Brown, L. D., Cai, T. T., and DasGupta, A. (2001). Interval estimation for a binomial proportion. *Stat.
573 Sci.*, 16(2):101–117.
- 574 D'Souza, R., Lysenko, M., and Rahmani, K. (2007). Sugarscape on steroids: simulating over a million
575 agents at interactive rates. In *Proc. of Agent 2007 Conf.*, Chicago, USA.
- 576 Edmonds, B. and Hales, D. (2003). Replication, replication and replication: Some hard lessons from
577 model alignment. *J. Artif. Soc. Soc. Simulat.*, 6(4).
- 578 Epstein, J. and Axtell, R. (1996). *Growing artificial societies: social science from the bottom up*. MIT
579 press.
- 580 Fachada, N. (2008). Agent-based simulation of the immune system. Master's thesis, Instituto Superior
581 Técnico, Universidade Técnica de Lisboa, Lisboa.
- 582 Fachada, N., Lopes, V. V., Martins, R. C., and Rosa, A. C. (2015a). Model-independent comparison of
583 simulation output. *arXiv*, 1509.09174. [cs.OH].
- 584 Fachada, N., Lopes, V. V., Martins, R. C., and Rosa, A. C. (2015b). Parallelization strategies for spatial
585 agent-based models. *arXiv*, 1507.04047. [cs.DC].
- 586 Gibbons, J. D. and Chakraborti, S. (2011). *Nonparametric statistical inference*. Springer.
- 587 Ginovart, M. (2014). Discovering the power of individual-based modelling in teaching and learning: The
588 study of a predator–prey system. *J. Sci. Educ. Technol.*, 23(4):496–513.
- 589 Goldsby, M. E. and Pancerella, C. M. (2013). Multithreaded agent-based simulation. In *Proceedings of
590 the 2013 Winter Simulation Conference: Simulation: Making Decisions in a Complex World*, WSC '13,
591 pages 1581–1591, Washington, D.C., USA. IEEE Press.
- 592 Grimm, V., Berger, U., DeAngelis, D., Polhill, J., Giske, J., and Railsback, S. (2010). The ODD protocol:
593 A review and first update. *Ecol. Model.*, 221(23):2760–2768.
- 594 Helbing, D. and Balmelli, S. (2012). How to do agent-based simulations in the future: from modeling
595 social mechanisms to emergent phenomena and interactive systems design. In *Social Self-Organization*,
596 chapter Agent-Based Modeling, pages 25–70. Springer.
- 597 Hiebeler, D. (1994). The Swarm simulation system and individual-based modeling. SFI Working Paper:
598 1994-11-065.
- 599 Isaac, A. G. (2011). The ABM template models: A reformulation with reference implementations. *J.
600 Artif. Soc. Soc. Simulat.*, 14(2):5.

- 601 Kahn, K. (2007). Comparing multi-agent models composed from micro-behaviours. In Rouchier, J., Cioffi-
602 Revilla, C., Polhill, G., and Takadama, K., editors, *M2M 2007: Third International Model-to-Model*
603 *Workshop*, Marseilles, France.
- 604 Kelton, W. D. (1997). Statistical analysis of simulation output. In *Proceedings of the 29th Conference on*
605 *Winter Simulation*, WSC '97, pages 23–30, Washington, DC, USA. IEEE Computer Society.
- 606 Law, A. M. (1983). Statistical analysis of simulation output data. *Oper. Res.*, 31(6):983–1029.
- 607 Law, A. M. (2007). Statistical analysis of simulation output data: the practical state of the art. In
608 *Simulation Conference, 2007 Winter*, pages 77–83. IEEE.
- 609 Law, A. M. (2015). *Simulation Modeling and Analysis*. McGraw-Hill, fifth edition.
- 610 Lotka, A. (1925). *Elements of Physical Biology*. Williams and Wilkins.
- 611 Lysenko, M. and D'Souza, R. (2008). A framework for megascale agent based model simulations on
612 graphics processing units. *J. Artif. Soc. Soc. Simulat.*, 11(4):10.
- 613 Lytinen, S. L. and Railsback, S. F. (2012). The evolution of agent-based simulation platforms: A review
614 of NetLogo 5.0 and ReLogo. In *Proceedings of the Fourth International Symposium on Agent-Based*
615 *Modeling and Simulation*.
- 616 Macal, C. and North, M. (2010). Tutorial on agent-based modelling and simulation. *J. Simulat.*, 4(3):151–
617 162.
- 618 Macal, C. M. and North, M. J. (2008). Agent-based modeling and simulation: ABMS examples. In
619 *Proceedings of the 40th Conference on Winter Simulation*, WSC '08, pages 101–112. Winter Simulation
620 Conference.
- 621 Martin, B. T., Zimmer, E. I., Grimm, V., and Jager, T. (2012). Dynamic energy budget theory meets
622 individual-based modelling: a generic and accessible implementation. *Methods Ecol. Evol.*, 3(2):445–
623 449.
- 624 Merlone, U., Sonnessa, M., and Terna, P. (2008). Horizontal and vertical multiple implementations in a
625 model of industrial districts. *J. Artif. Soc. Soc. Simulat.*, 11(2):5.
- 626 Müller, B., Balbi, S., Buchmann, C. M., De Sousa, L., Dressler, G., Groeneveld, J., Klassert, C. J., Le,
627 Q. B., Millington, J. D., Nolzen, H., et al. (2014). Standardised and transparent model descriptions for
628 agent-based models: Current status and prospects. *Environ. Model. Softw.*, 55:156–163.
- 629 Nakayama, M. K. (2008). Statistical analysis of simulation output. In *Proceedings of the 40th Conference*
630 *on Winter Simulation*, WSC '08, pages 62–72. Winter Simulation Conference.
- 631 Ottino-Loffler, J., Rand, W., and Wilensky, U. (2007). Co-evolution of predators and prey in a spatial
632 model. In *GECCO 2007*.
- 633 Park, H. M. (2008). Univariate analysis and normality test using SAS, Stata, and SPSS. Working
634 Paper. The University Information Technology Services (UITS) Center for Statistical and Mathematical
635 Computing, Indiana University.
- 636 Radax, W. and Rengs, B. (2010). Prospects and pitfalls of statistical testing: Insights from replicating the
637 demographic prisoner's dilemma. *J. Artif. Soc. Soc. Simulat.*, 13(4):1.
- 638 Railsback, S., Lytinen, S., and Grimm, V. (2005). *StupidModel and extensions: A template and teaching*
639 *tool for agent-based modeling platforms*. Swarm Development Group.
- 640 Railsback, S., Lytinen, S., and Jackson, S. (2006). Agent-based simulation platforms: Review and
641 development recommendations. *Simulation*, 82(9):609–623.
- 642 Razali, N. M. and Wah, Y. B. (2011). Power comparisons of Shapiro-Wilk, Kolmogorov-Smirnov,
643 Lilliefors and Anderson-Darling tests. *J. Stat. Model. Anal.*, 2(1):21–33.
- 644 Reynolds, C. (2006). Big fast crowds on PS3. In *Proceedings of the 2006 ACM SIGGRAPH Symposium*
645 *on Videogames*, Sandbox '06, pages 113–121, New York, NY, USA. ACM.
- 646 Reynolds, C. W. (1987). Flocks, herds and schools: A distributed behavioral model. *SIGGRAPH Comput.*
647 *Graph.*, 21(4):25–34.
- 648 Rollins, N. D., Barton, C. M., Bergin, S., Janssen, M. A., and Lee, A. (2014). A computational model
649 library for publishing model documentation and code. *Environ. Model. Softw.*, 61:59–64.
- 650 Sallach, D. and Mellarkod, V. (2005). Interpretive agents: A heatbug reference simulation. In *Proc. Agent*
651 *2005 Conf. Generative Social Processes, Models, and Mechanisms*, pages 693–705.
- 652 Sanchez, S. M. (1999). ABC's of output analysis. In *Simulation Conference Proceedings, 1999 Winter*,
653 volume 1, pages 24–32, Phoenix, AZ, USA. IEEE.
- 654 Sargent, R. G. (1976). Statistical analysis of simulation output data. *SIGSIM Simul. Dig.*, 7(4):39–50.
- 655 Shapiro, S. S. and Wilk, M. B. (1965). An analysis of variance test for normality (complete samples).

- 656 *Biometrika*, 52(3/4):591–611.
- 657 Shook, E., Wang, S., and Tang, W. (2013). A communication-aware framework for parallel spatially
658 explicit agent-based models. *Int. J. Geogr. Inf. Sci.*, 27(11):2160–2181.
- 659 Smith, M. (1991). Using massively-parallel supercomputers to model stochastic spatial predator-prey
660 systems. *Ecol. Model.*, 58(1):347–367.
- 661 Sondahl, F., Tisue, S., and Wilensky, U. (2006). Breeding faster turtles: Progress towards a NetLogo
662 compiler. In *Proceedings of the Agent 2006 conference on social agents, Chicago, IL, USA*.
- 663 Standish, R. K. (2008). Going stupid with EcoLab. *Simulation*, 84(12):611–618.
- 664 Tang, W. and Wang, S. (2009). HPABM: A hierarchical parallel simulation framework for spatially-explicit
665 agent-based models. *Trans. GIS*, 13(3):315–333.
- 666 Tatara, E., North, M., Howe, T., Collier, N., Vos, J., and Vos, J. (2006). An introduction to Repast modeling
667 using a simple predator-prey example. In Sallach, D., Macal, C., and M.J., N., editors, *Proceedings of
668 the Agent 2006 Conference on Social Agents: Results and Prospects*, volume ANL/DIS-06-7, pages
669 83–94. co-sponsored by the Argonne National Laboratory and The University of Chicago.
- 670 Volterra, V. (1926). Fluctuations in the abundance of a species considered mathematically. *Nature*,
671 118:558–560.
- 672 Welch, P. D. (1981). On the problem of the initial transient in steady-state simulation. IBM Watson
673 Research Center.
- 674 Wilensky, U. (1997). NetLogo wolf sheep predation model.
- 675 Wilensky, U. (1999). NetLogo.
- 676 Wilensky, U. (2004). NetLogo heatbugs model.
- 677 Wilensky, U. (2014). *NetLogo 5.1.0 User Manual*. Northwestern University, Evanston, IL, USA.
- 678 Wilensky, U. and Rand, W. (2007). Making models match: replicating an agent-based model. *J. Artif.
679 Soc. Soc. Simulat.*, 10(4):2.
- 680 Willink, R. (2005). A confidence interval and test for the mean of an asymmetric distribution. *Commun.
681 Stat. Theor. M.*, 34(4):753–766.

1

NetLogo implementation of the PPHPC model.

Figure 1. NetLogo implementation of the PPHPC model.

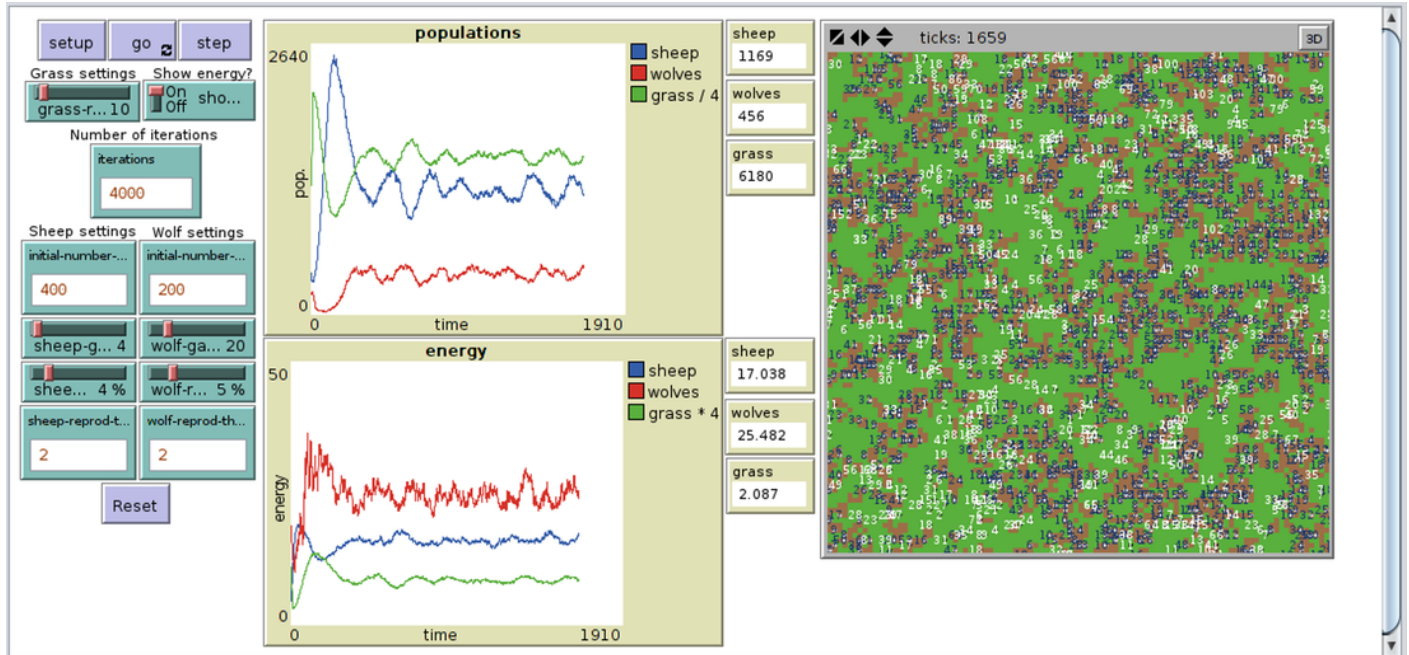


Figure 2(on next page)

Moving average of outputs for model size 400 with $w=10$

Moving average of outputs for model size 400 with $w=10$. Other model sizes produce similar results, apart from a vertical scaling factor. The dashed vertical line corresponds to iteration l after which the output is considered to be in steady-state. (A) Population moving average, param. set 1. (B) Energy moving average, param. set 1. (C) Population moving average, param. set 2. (D) Energy moving average, param. set 2.

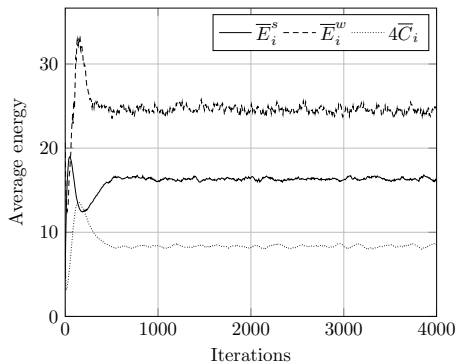
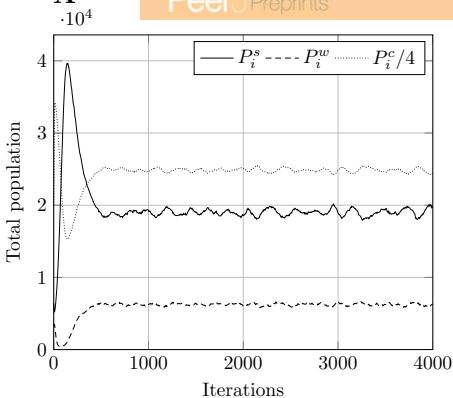
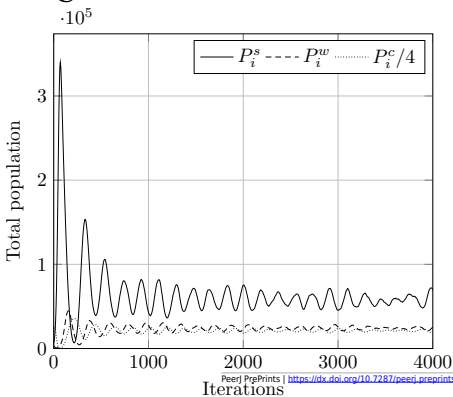
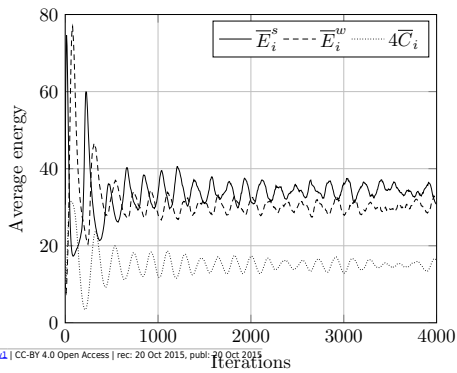
A**B****C****D**

Figure 3(on next page)

Typical model output for model size 400

Figure 2. Typical model output for model size 400. Other model sizes have outputs which are similar, apart from a vertical scaling factor. P_i refers to total population, $\text{mean}\{E\}_i$ to mean energy and $\text{mean}\{C\}_i$ to mean value of the countdown state variable, C .

Superscript ss relates to prey, w to predators, and c to cell-bound food. P_i^{c} and $\text{mean}\{C\}_i$ are scaled for presentation purposes. (A) Population, param. set 1. (B) Energy, param. set 1. (C) Population, param. set 2. (D) Energy, param. set 2.

